

CHEMISTRY

Thin adhesive oil films lead to anomalously stable mixtures of water in oil

Claire Nannette^{1,2}, Jean Baudry¹, Anqi Chen³, Yiqiao Song^{3,4}, Abdulwahed Shglabow¹, Nicolas Bremond¹, Damien Démoulin², Jamie Walters², David A. Weitz^{3,5,6}, Jérôme Bibette^{1*}

Oil and water can only be mixed by dispersing droplets of one fluid in the other. When two droplets approach one another, the thin film that separates them invariably becomes unstable, causing the droplets to coalesce. The only known way to avoid this instability is through addition of a third component, typically a surfactant, which stabilizes the thin film at its equilibrium thickness. We report the observation that a thin fluid film of oil separating two water droplets can lead to an adhesive interaction between the droplets. Moreover, this interaction prevents their coalescence over timescales of several weeks, without the use of any surfactant or solvent.

Oil and water do not mix. When the two are violently shaken together, droplets of one fluid will form inside the other, but when two droplets are brought in close proximity to one another, they are unstable and will coalesce to form a single droplet. As the interfaces approach one another, the intervening fluid layer becomes very thin and thermally induced capillary waves on each interface lead to merging (1). This can only be avoided through the addition of a third component, a surfactant, which induces a repulsive interaction that prevents spontaneous coalescence because of capillary waves, except in highly specific cases such as water-in-liquid-crystal emulsions (2), some very dilute charged systems (3), or when some intrinsic impurities can act as surfactant (4). Instead, coalescence can only occur in the thin fluid film separating the droplets through a thermally activated nucleation of a hole that must reach a critical size above which it becomes unstable (5). The activation energy for nucleation of a hole can be large, leading to long-term stability of the surfactant-stabilized droplets. In some cases there can be an attractive interaction, which causes droplets to adhere to one another while still retaining their integrity because of the adsorbed surfactant (6). For example, a classic example of this phenomenon takes place when oil droplets in water, commonly called direct emulsions, are stabilized by a widely used surfactant such as SDS (sodium dodecyl sul-

fate). The addition of excess salt causes interfaces of neighboring droplets to wet one another, resulting in a very thin water film separating the droplets (7). This leads to adhesion, but the stability of the droplets is retained. Similar behavior can be observed for water droplets in oils, commonly called inverse emulsions: Addition of a solvent to the oil can cause the surfactant stabilizing the droplets to become less soluble in the continuous phase and hence induce an attractive interaction that leads the droplets to wet one another; nevertheless, coalescence is still avoided because of the surfactant (8, 9). Attractive

interactions between droplets can only occur when molecules at the interface of the droplets are more compatible with one another than with the solvent itself. In all cases, stability of a thin oil film separating two water droplets can only be achieved through the incorporation of one or more additional components able to adsorb at the interfaces (10).

We report the spontaneous formation of an anomalously stable thin film of oil between droplets of water for a polymeric oil. When there is weak adsorption of the oil on the water interface, the oil molecules at the interface become less compatible with the bulk oil, resulting in a weak attractive interaction between the two water droplets that induces a dramatic change in the dynamics of the oil molecules within the thin film. As a result, the water droplets can remain stable over large timescales, even in the absence of surfactant or any other additional components whatsoever. By measuring the temperature dependence of this stability, we show that it results from an increase by seven orders of magnitude in the effective viscosity of the oil in the thin adhesive films between the droplets, as compared with the bulk viscosity. As a consequence, stable water-in-oil emulsions can be produced in the absence of surfactant even at very high volume fractions of water. Moreover, because of this unexpected metastability, above a characteristic water volume fraction, ϕ^* , the emulsion breaks under shear and spontaneously

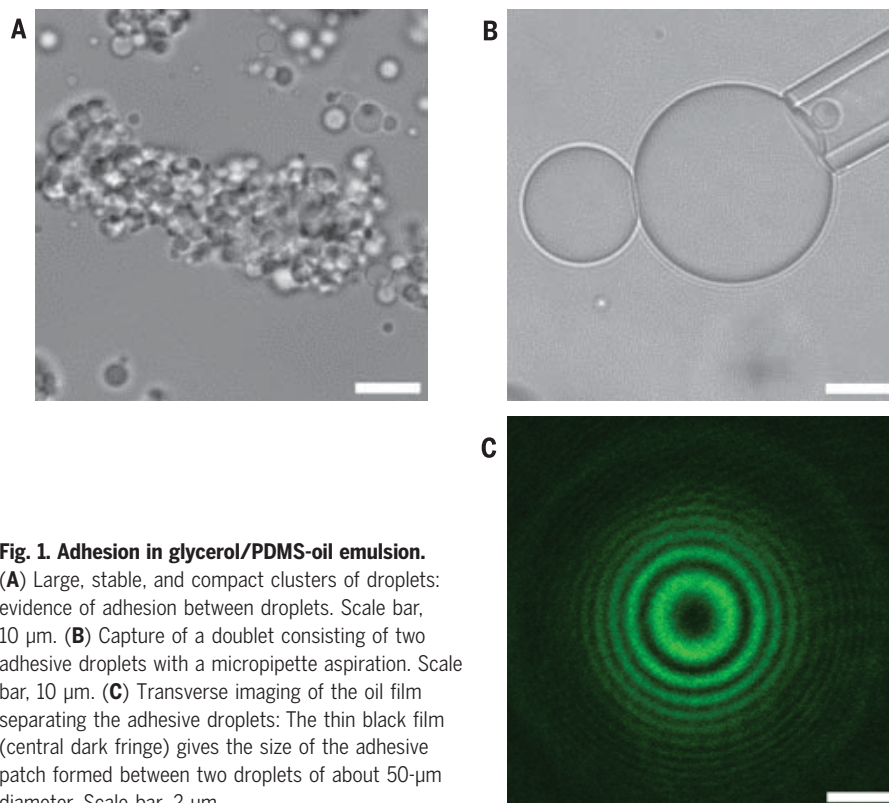


Fig. 1. Adhesion in glycerol/PDMS-oil emulsion.

(A) Large, stable, and compact clusters of droplets: evidence of adhesion between droplets. Scale bar, 10 μm . (B) Capture of a doublet consisting of two adhesive droplets with a micropipette aspiration. Scale bar, 10 μm . (C) Transverse imaging of the oil film separating the adhesive droplets: The thin black film (central dark fringe) gives the size of the adhesive patch formed between two droplets of about 50- μm diameter. Scale bar, 2 μm .

¹Laboratoire Colloïdes et Matériaux Divisés, CBI, ESPCI Paris, Université PSL, CNRS, 75005 Paris, France. ²Calyxia, 94380 Bonneuil-sur-Marne, France. ³John A. Paulson School of Engineering and Applied Sciences, Harvard University, Cambridge, MA 02138, USA. ⁴Athinoula A. Martinos Center for Biomedical Imaging, Department of Radiology, Massachusetts General Hospital, Charlestown, MA 02129, USA. ⁵Department of Physics, Harvard University, Cambridge, MA 02138, USA. ⁶Wyss Institute for Biologically Inspired Engineering, Harvard University, Boston, MA 02215, USA.

*Corresponding author. Email: jerome.bibette@espci.fr

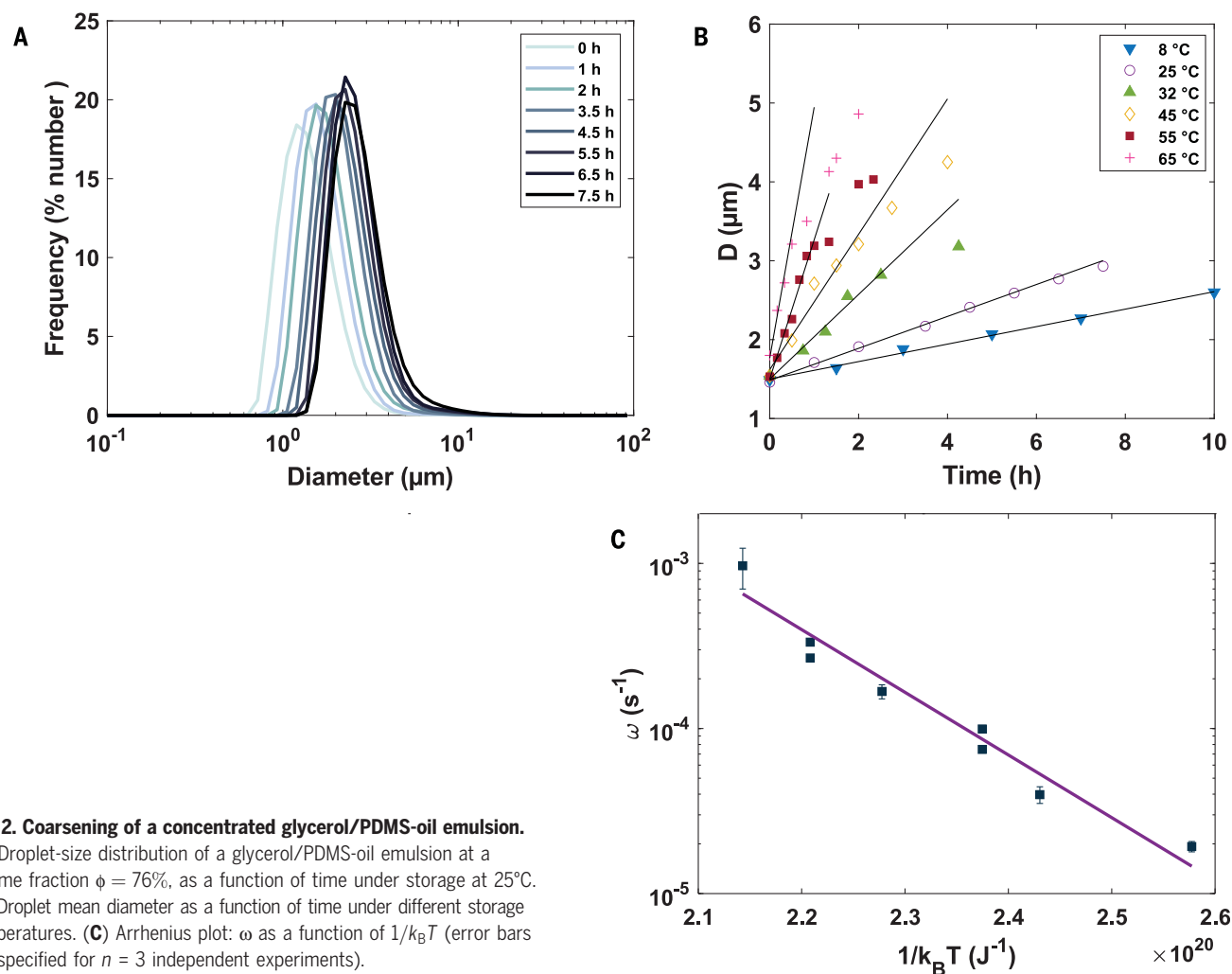


Fig. 2. Coarsening of a concentrated glycerol/PDMS-oil emulsion. (A) Droplet-size distribution of a glycerol/PDMS-oil emulsion at a volume fraction $\phi = 76\%$, as a function of time under storage at 25°C. (B) Droplet mean diameter as a function of time under different storage temperatures. (C) Arrhenius plot: ω as a function of $1/k_B T$ (error bars are specified for $n = 3$ independent experiments).

forms double-emulsion globules consisting of the primary water-in-oil dispersion.

Adhesion of stable oil films separating water interfaces

To illustrate this phenomenology, we investigated the behavior of a pure binary mixture of glycerol and polydimethylsiloxane (PDMS) (fig S1). We mixed glycerol ($\eta_g = 0.84$ Pa.s) into PDMS oil [weight-average molecular weight (M_w) = 30,000 g/mol] (12) with a viscosity of $\eta_0 = 1$ Pa.s to form glycerol droplets of diameter D of about 2 μm [supplementary materials (SM), methods 1]. As the droplets approach one another, instead of coalescing, they stick to each other while still retaining their integrity (Fig. 1A). The existence of these compact clusters indicates that there must be an adhesive interaction between droplets. To confirm this, we used micropipette aspiration to immobilize a doublet consisting of one droplet adhering to a second (SM, methods 2). The two droplets adhere to one another,

demonstrating the attractive interaction (Fig. 1B). To measure this attractive interaction, we illuminated the interface between two droplets with a laser and analyzed the resultant interference pattern (12). The adhesive patch causes a black central circle in the interference pattern (Fig. 1C). The size of this circle enabled us to determine the diameter of the adhesive patch (7), a , from which we deduced the contact angle of the adhesive droplets, θ , which we found to be $\theta = 2^\circ$ (SM, methods 3, and supplementary text) (13). By determining the surface tension between glycerol and PDMS, $\gamma = 25$ mJ/m², we were able to determine the adhesive energy (14), $\varepsilon = 2\gamma(1 - \cos\theta)$, which gives $\varepsilon = 3 \times 10^{-2}$ mJ/m². For two identical droplets, if $\varepsilon/\gamma \ll 1$, the diameter of the adhesive patch must scale with the diameter of the drop as $(a/D)^2 = \varepsilon/\gamma$ (6). Although the area of each adhesive patch is very small, coalescence must take place within the patches because the contact angle leads to further separation of neighboring interfaces.

Origin of the stability of the thin oil films

To quantify the stability of these thin adhesive oil films, we measured the time evolution of the size distribution of droplets resulting from coalescence, which is the dominant mechanism of coarsening (movie S1). We used an emulsion with a volume fraction, $\phi = 76\%$, which is high enough to preclude any considerable relative motion of the droplets, ensuring that the measured coalescence rate reflects only the intrinsic instability of the thin films separating droplets in contact with one another (15). We determined the number-averaged size distribution (SM, methods 4), which maintains a constant shape, whereas the mean size increases with time (Fig. 2A). To probe the nature of the metastability of the thin oil film, we measured the temperature dependence of the evolution of the mean diameter: For each temperature, T , the initial time dependence of D is linear, whereas the rate of growth increases markedly with increasing T (Fig. 2B). The frequency of coalescence, ω , is

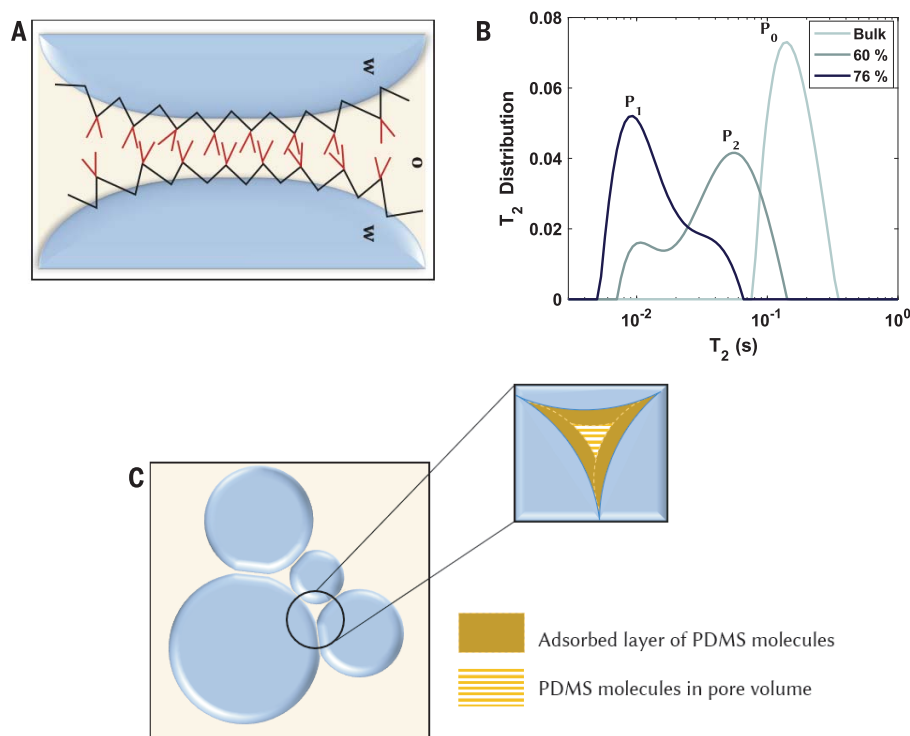


Fig. 3. Specific adsorption of oil molecules at the interface. (A) Schematic representation of the interaction mechanism between PDMS oil/glycerol interfaces: The hydrophobic moieties of the oil (methyl group in red) specifically adhere, whereas the hydrophilic parts of the backbone (black lines) composed of oxygen atoms are preferentially adsorbed on the glycerol surface; this may account for the attraction between the droplets. w, water; o, oil. (B) Plot of T_2 relaxation-time distribution as a function of time for PDMS used as the continuous phase of a glycerol/PDMS-oil emulsion compared with its bulk value. The bimodal T_2 distribution indicates that within the emulsion, PDMS molecules are of two types: One is confined in the thin film; the other is trapped in the Plateau borders of the emulsion. (C) Schematic representation of the pore surrounded by droplets, the so-called Plateau border: The PDMS contained in Plateau borders is either located in the adsorbed layer or confined in this pore volume.

proportional to the rate of growth normalized by the initial drop diameter. We found that $\log \omega$ depends linearly on the inverse of T (Fig. 2C). Thus, the coarsening exhibits an Arrhenius behavior given by $\omega = \omega_0 e^{-E_a/k_B T}$, where ω_0 is the attempt frequency, k_B is Boltzmann's constant, and E_a is the energy barrier for the nucleation of a hole of critical radius r^* in the thin film separating two droplets, which induces coalescence. From the slope of the data, we determined $E_a = 20 k_B T$, with $T = 298$ K. By comparison, surfactant-stabilized emulsions typically exhibit a much higher energy barrier of at least $30 k_B T$ (16).

To determine the value of r^* , we used the simplest model of nucleation and growth, the capillary model (17). The energy, $E(r)$, of a hole of radius r , is $E(r) = -2\pi r^2 \gamma + 2\pi r \Gamma$, where γ is the surface tension and Γ is the line tension, which accounts for all contributions associated with the inherent high curvature along the perimeter of the hole (supplementary text). This leads to $r^* = \left(\frac{E_a}{2\pi\gamma}\right)^{1/2}$, and we obtain $2r^* = 1.4$ nm. From this value, we could also infer the thickness of the film, h , which, as assumed by the

capillary model, must be of the same order of magnitude, a few nanometers (18).

Further insight into the nature of this behavior comes from determining the attempt frequency, $\omega_0 \sim 10^5$ s $^{-1}$, which is obtained from the intercept of the fit to the data in Fig. 2C. The nucleation rate of a hole (19), k_0 , is determined by a balance between surface tension—which drives the growth of the hole—and the viscosity of the oil in the film, which slows the growth, $k_0 \sim \frac{\gamma}{\eta r^*}$. The value of ω_0 is determined by k_0 normalized by the number of holes possible, $\omega_0 = k_0 \frac{s}{r^{s/2}}$, where s is the specific surface area of one drop in contact with its neighboring droplets, where coalescence must occur. Each drop is surrounded on average by a number, z , of neighboring droplets. Therefore, the fraction of the drop surface occupied by adhesive patches is $z \left(\frac{a}{D}\right)^2$, which is about 1% of the drop surface if we assume $z = 10$, as expected for a densely packed emulsion. Thus, within the thin adhesive film, the effective viscosity of the oil, η_{eff} , must be a factor of $\sim 10^7$ more than η_0 (fig. S2). It is this large increase in the viscosity in the thin film

where coalescence takes place that compensates for the relatively low activation energy and leads to this stable thin adhesive film. The uncertainty of this estimate is about an order of magnitude, given the uncertainty in the determination of ω_0 and k_0 .

Molecular nature of the thin oil films

We must therefore consider the nature of this thin adhesive film more carefully. A PDMS molecule at a hydrophilic interface spreads and forms a nanometer-thick layer (20, 21). The preferential adsorption of the oxygen along the PDMS backbone leads to an excess of hydrophilicity at the glycerol interface; this must be compensated by an excess of hydrophobicity localized on the opposite side, as shown schematically in Fig. 3A. Thus, two identical mirror-image layers will weakly adhere to one another instead of remaining surrounded by bulk oil molecules. For a glycerol-PDMS interface in contact with its mirror image, the entire film tension is lowered by $\epsilon/2$, which is much smaller than γ . Although this energy is relatively small, we hypothesized that it nevertheless creates patches within which the molecular dynamics are severely affected, leading to the very large increase in effective viscosity. Van der Waals interactions could also contribute to the adhesion energy that we measured; however, the persistence of the thin adhesive film reflects the existence of a short-range repulsion that must be set solely by an interplay between chain adsorption and adhesion of hydrophobic moieties (supplementary text). Moreover, because this mechanism is molecular in scale, the thickness of these thin films must also be molecular in scale in agreement with measurement on a single interface and in accord with the value deduced by the capillary model (17, 18).

To explore the molecular basis of this hypothesis, we performed nuclear magnetic resonance (^1H NMR) measurements on concentrated glycerol-PDMS emulsions with ϕ between 60 and 76% (SM, methods 5). We focused on the spin-spin relaxation time (T_2) of the PDMS, which reflects its molecular motion (22). For the most concentrated emulsion, $\phi = 76\%$, we observed a pronounced peak, P_1 , in the T_2 relaxation-time distribution, centered around 9×10^{-3} s, which is a factor of 14 less than the peak, P_0 , for the same PDMS in the absence of any glycerol. There is, in addition, a second peak, P_2 , which appears as a shoulder around 5×10^{-2} s (Fig. 3B). When the volume fraction is decreased to $\phi = 60\%$, P_1 has a smaller amplitude but remains at nearly the same position, while P_2 becomes more pronounced and shifts toward P_0 (Fig. 3B).

To account for these NMR results, we hypothesized that there are two types of PDMS molecules within the concentrated emulsion: One type has slow dynamics, and thus

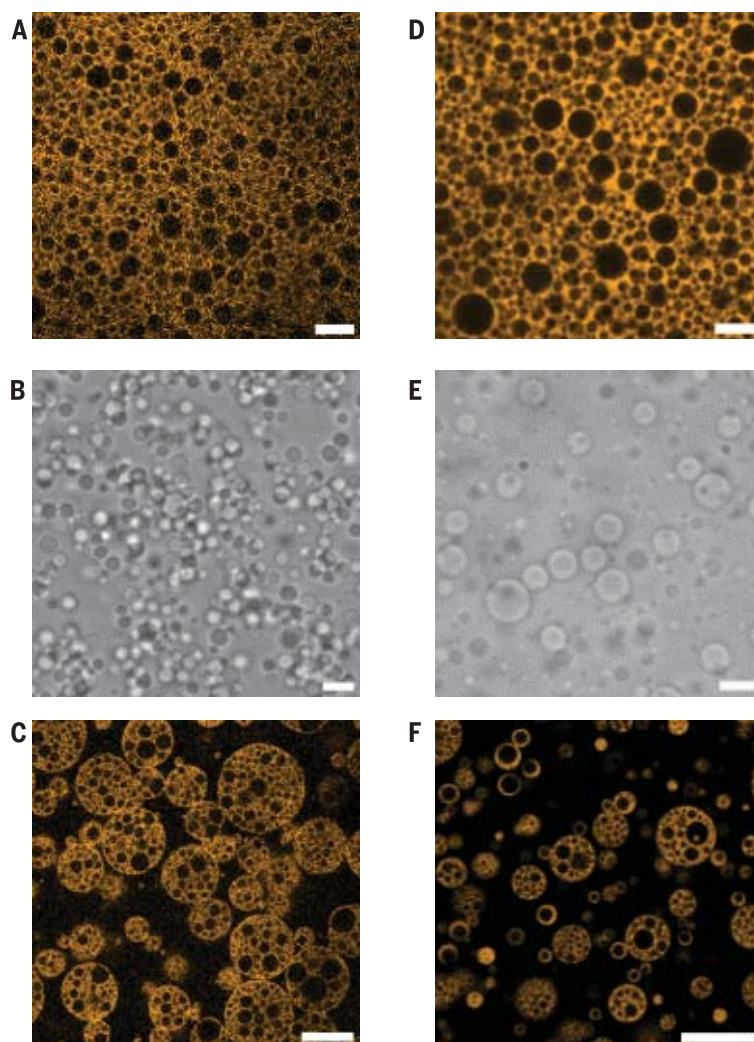
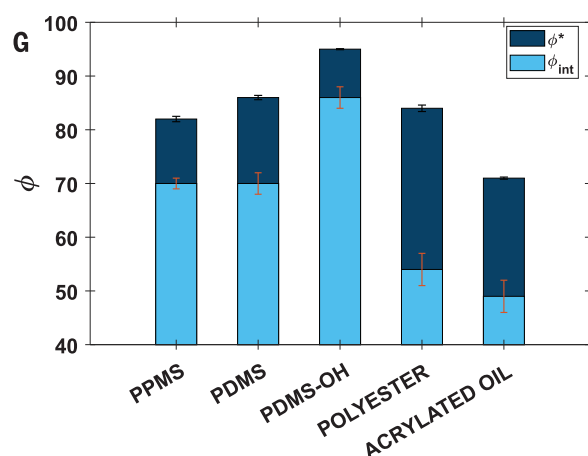


Fig. 4. Emulsions formed with different oils without surfactants.

(A) A stable emulsion of glycerol in hydroxy-terminated PDMS oil (dyed orange) can be prepared at higher ϕ of 80%. Scale bar, 5 μm . (B) Microscopic picture of a diluted glycerol in hydroxy-terminated PDMS oil emulsion: evidence for compact connected clusters. Scale bar, 5 μm . (C) Double emulsion obtained with the hydroxy-terminated PDMS oil after phase inversion at $\phi^* = 95\%$. Scale bar, 10 μm . (D) A stable emulsion of glycerol in acrylated vegetable oil (dyed orange) can be prepared at ϕ of 70%. Scale bar, 5 μm . (E) Adhesion is also evidenced in a diluted glycerol in acrylated vegetable oil emulsion. Scale bar, 5 μm . (F) Double emulsion obtained with the acrylated vegetable oil after phase inversion at $\phi^* = 71\%$. Globules are less concentrated in internal phase because $\phi_{\text{int}} = 49\%$. Scale bar, 10 μm . (G) Critical volume fraction ϕ^* at which inversion takes place and internal fraction of glycerol within double globule, ϕ_{int} ; both fractions depend on the chosen water/oil couple only ($n = 3$; SM, methods 5).



short T_2 , which is nearly independent of ϕ , as shown by the position of P_1 , which remains approximately constant as ϕ changes. The other type has faster dynamics and thus longer T_2 , but does change with ϕ . We hypothesized that the first type represents PDMS molecules that are located in the direct vicinity of the thin adhesive film separating droplets, whereas the second type represents PDMS molecules that are located in the Plateau borders and includes both the molecules within the pore and those adsorbed on the pore surface but not in direct vicinity of the adhesive patches (Fig. 3C). Because the average dynamics of molecules within a pore include contributions from both the oil molecules adsorbed on the glycerol interface and the oil molecules confined within the pore, the peak position should change with ϕ as the relative amount of PDMS adsorbed to the interface changes with the change in pore size; this is indeed what we observed for P_2 , which is consistent with our hypothesis. By

contrast, the dynamics of the PDMS molecules in the vicinity of the thin adhesive film include contributions from those molecules confined within the adhesive patch itself and some molecules in close proximity to it. The structure and size of these thin films are preserved by the adhesive forces, independent of dilution. Therefore, the position of the P_1 peak, which is associated with them, should not change with ϕ . However, its amplitude should decay because the proportion of thin films decreases as ϕ decreases. This is indeed what we observed for P_1 , which is consistent with our hypothesis (supplementary text). For the highest water volume fraction, $\phi = 76\%$, the T_2 value of P_1 corresponds to an effective viscosity (23) $\eta_{\text{eff}} \approx 10^4 \eta_0$; this must reflect contributions of the strongly adhesive molecules directly in the film itself and the neighboring molecules whose motion is restricted but not as strongly. Thus, these molecular-scale NMR results exhibit a trend that is consistent with the large increase

in η_{eff} determined from the analysis of the hole-nucleation attempt frequency.

Evidence of a generic metastability mechanism

The observation of stable oil films extends beyond this PDMS oil. We produced emulsions with several different oils and hydrophilic phases; each emulsion remained stable. For the aqueous phase, we used either glycerol or water with the addition of a few percent sodium alginate so as to match the oil viscosity to optimize emulsification. For each combination, we measured the characteristic water volume fraction at which the emulsion breaks under shear and spontaneously forms double-emulsion globules consisting of the primary water-in-oil dispersion. This provided a convenient comparison among different fluid pairs. In all cases, ϕ^* depends only on the specific choice of the fluids and not on how they are mixed. Moreover, in all cases, after dilution, we

observed clusters reflecting an attractive interaction between the droplets.

We first compared the behavior of hydroxy-terminated PDMS of the same molecular weight with that of the methyl-terminated PDMS oil. Although this is a very slight modification in the molecular structure, which corresponds to the replacement of only two methyl groups out of approximately 600, it nevertheless induces a large change in ϕ^* : Highly packed emulsions remain stable at even higher volume fractions, up to $\phi^* = 95\%$ (Fig. 4A). Upon dilution, we observed the presence of large and dense clusters, which reflects an even stronger adhesive interaction (Fig. 4B). Above ϕ^* , the emulsion breaks under shear into a double emulsion consisting of globules with an internal glycerol volume fraction $\phi_{\text{int}} = 86\%$ (SM, methods 6) and with somewhat-larger water droplets (Fig. 4C). We also made stable emulsions using acrylated vegetable oils; a fluorescent image of such an emulsion with $\phi = 70\%$ is shown in Fig. 4D. In contrast to the PDMS oils, these emulsions have a lower ϕ^* of 71%. Upon dilution, we observed much smaller clusters, reflecting a weaker adhesive interaction between interfaces (Fig. 4E). Above ϕ^* , the emulsion breaks into a double emulsion consisting of globules with noticeably larger water droplets (Fig. 4F). This acrylated oil has a polymeric backbone (fig. S3), which should lead to weaker adsorption and hence lower adhesion, which is consistent with the smaller clusters observed upon dilution. We summarize the values of ϕ^* and ϕ_{int} for PDMS, hydroxy PDMS, acrylated vegetable oil, and polyester oil in Fig. 4G. Further exploration of which oils make stable inverse emulsions with either pure water, water with sodium alginate, or glycerol shows that (i) silicone oil and all its derivatives including amine and phenyl substituted chains produce stable emulsions, provided that oil has a polymeric character with a molecular weight exceeding about 5000g/mol, and that (ii) polyurethane oils and polyester oils (including their derivatives) also exhibit stable water-in-oil emulsions (fig. S3).

These findings demonstrate the unexpected behavior of a polymeric oil when it adsorbs on

the interface of a hydrophilic liquid and becomes confined in a very thin film. An inherent consequence of this weak binding of polymeric oils to the water interface, which is due to their slightly polar nature, is their conformational change, exposing a more hydrophobic portion of the molecule toward the bulk oil. This results in a weak adhesion between two identical interfaces and leads to a dramatic increase in the effective viscosity of the oil in the thin film as compared with its bulk value; such an effect has been observed so far only on a solid surface (24, 25). In the case of a liquid interface, it must be understood as an intrinsic consequence of both adsorption and adhesion, which together efficiently modify the polymer dynamics at liquid interfaces as a direct consequence of the counterintuitive lowering of the interfacial free energy.

Conclusions

These results represent a mechanism for stabilizing water droplets in oil in the absence of surfactant. They also represent an important route to formulating materials through double emulsions made in a single step (26, 27). When ϕ exceeds ϕ^* , the emulsion breaks under shear, forming a double emulsion without the use of any surfactant nor any solvent whatsoever. This finding will have important technological applications: It enables the creation of very pure and controlled materials, particularly for polymerizable oils such as those used in this study.

REFERENCES AND NOTES

1. E. Chatzigiannakis, J. Vermant, *Phys. Rev. Lett.* **125**, 158001 (2020).
2. P. Poulin, H. Stark, T. C. Lubensky, D. A. Weitz, *Science* **275**, 1770–1773 (1997).
3. J. K. Beattie, A. M. Djerdjev, *Angew. Chem. Int. Ed.* **43**, 3568–3571 (2004).
4. K. Roger, B. Cabane, *Angew. Chem. Int. Ed.* **51**, 5625–5628 (2012).
5. A. Kabalnov, H. Wennerström, *Langmuir* **12**, 276–292 (1996).
6. P. Poulin, J. Bibette, *Phys. Rev. Lett.* **79**, 3290–3293 (1997).
7. P. Poulin, F. Nallet, B. Cabane, J. Bibette, *Phys. Rev. Lett.* **77**, 3248–3251 (1996).
8. P. Poulin, J. Bibette, *Langmuir* **14**, 6341–6343 (1998).
9. A. R. Thiam, N. Bremond, J. Bibette, *Langmuir* **28**, 6291–6298 (2012).
10. D. Langevin, *Langmuir* **39**, 3821–3828 (2023).
11. K. Mojsiewicz-Pienkowska, *J. Pharm. Biomed. Anal.* **58**, 200–207 (2012).

12. B. Hogan, A. Babataheri, Y. Hwang, A. I. Barakat, J. Husson, *Biophys. J.* **109**, 209–219 (2015).
13. H. M. Princen, *Colloids Surf.* **9**, 47–66 (1984).
14. M. P. Aronson, H. M. Princen, *Nature* **286**, 370–372 (1980).
15. V. Schmitt, F. Leal-Calderon, *Europhys. Lett.* **67**, 662–668 (2004).
16. K. Pays, J. Giermanska-Kahn, B. Poulin, J. Bibette, F. Leal-Calderon, *Phys. Rev. Lett.* **87**, 178304 (2001).
17. A. B. Croll, K. Dalnoki-Veress, *Soft Matter* **6**, 5547–5553 (2010).
18. M. Ilton, C. DiMaria, K. Dalnoki-Veress, *Phys. Rev. Lett.* **117**, 257801 (2016).
19. B. Deminiere, A. Colin, F. Leal-Calderon, J. F. Muzy, J. Bibette, *Phys. Rev. Lett.* **82**, 229–232 (1999).
20. A. E. Ismail, G. S. Grest, D. R. Heine, M. J. Stevens, M. Tsige, *Macromolecules* **42**, 3186–3194 (2009).
21. C. Kim, M. C. Gurau, P. S. Cremer, H. Yu, *Langmuir* **24**, 10155–10160 (2008).
22. J. P. Cohen-Addad, M. Domard, S. Boileau, *J. Chem. Phys.* **75**, 4107–4114 (1981).
23. J. Götz, H. Weisser, S. Altmann, "Correlation of the Viscosity and the Molecular Weight of Silicone Oils with the T2 NMR Relaxation Times" in *Organosilicon Chemistry V: From Molecules to Materials*, N. Auner, J. Weis, Eds. (Wiley-VCH Verlag GmbH, 2003), pp. 584–594.
24. Z. Yang, Y. Fujii, F. K. Lee, C.-H. Lam, O. K. C. Tsui, *Science* **328**, 1676–1679 (2010).
25. J. Klein, E. Kumacheva, *Science* **269**, 816–819 (1995).
26. J. A. Hanson et al., *Nature* **455**, 85–88 (2008).
27. Z. Li et al., *Langmuir* **30**, 12154–12163 (2014).

ACKNOWLEDGMENTS

Funding: This research was supported by Calyxia (CN) Capsum Institut Pierre-Gilles de Gennes (Équipement d'Excellence, "Investissements d'avenir," program ANR-10- EQPX-34) and by the NSF through the Harvard Materials Research Science and Engineering Center (MRSEC, DMR-2011754). **Author contributions:** Conceptualization: C.N., D.D., J.W., N.B., J.Ba., and J.Bi. Methodology: C.N., N.B., J.Ba., and J.Bi. Investigation: C.N., A.C., Y.S., and A.S. Visualization: C.N., A.C., Y.S., N.B., J.Ba., D.A.W., and J.Bi. Writing – original draft: C.N., J.Ba., and J.Bi. Writing – review and editing: C.N., N.B., J.Ba., D.A.W., and J.Bi. **Competing interests:** C.N., D.D., J.Ba., and J.Bi. hold patents related to this work (European unexamined patent application EP22305808 and French unexamined patent application FR2306227). D.A.W. and J.Bi. are co-founders and shareholders of Calyxia. D.A.W. and J.Bi. have advisory activities for Calyxia. **Data and materials availability:** All data are available in the main text or the supplementary materials. **License information:** Copyright © 2024 the authors, some rights reserved; exclusive licensee American Association for the Advancement of Science. No claim to original US government works. <https://www.science.org/about/science-licenses-journal-article-reuse>

SUPPLEMENTARY MATERIALS

science.org/doi/10.1126/science.adj6728
Materials and Methods
Supplementary Text
Figs. S1 to S3
References (28–35)
Movie S1

Submitted 10 July 2023; accepted 6 March 2024
10.1126/science.adj6728